SUPPORTING INFORMATION FOR:

Physically crosslinked polybutadiene by quadruple hydrogen bonding through side-chain incorporation of ureidopyrimidinone with branched alkyl side chains

Jente Verjans,[1] Alexis André,[2,3] Evelyne Van Ruymbeke,[2] and Richard Hoogenboom[1,*]

[1] Supramolecular Chemistry Group, Centre of Macromolecular Chemistry (CMaC), Department of Organic and Macromolecular Chemistry, Ghent University, B-9000 Ghent, Belgium.

[2] Bio- and Soft Matter, Institute of Condensed Matter and Nanosciences, Université catholique de Louvain, B-1348 Louvain-la-Neuve, Belgium.

[3] Department of Chemical Engineering, Katholieke Universiteit Leuven, B-3001 Leuven, Belgium.

Table of contents

Figure S1: DOSY NMR spectrum of PB-U4 S2

Figure S2: DOSY NMR spectrum of PB-U8 S2

Figure S3: DOSY NMR spectrum of PB-U13 S3

Figure S4: TGA curves of all PB-UPy polymers S3

Figure S5: PB-UPy films obtained after compression molding S4

Figure S6: Test of time−temperature superposition at T_{ref} = 80 °C S4

Figure S7: Test of time−temperature superposition at T_{ref} = 60 °C S5

Figure S8: Scaling laws of the storage modulus for (ϵ>1) and (0<ϵ<1) S5

Figure S9: Predictions of the sticky Rouse model (with the loops) for the system PB-U6 S6

Figure S10: Predictions of the sticky Rouse model (with the loops) for the system PB-U8 S6

Figure S11: Predictions of the sticky Rouse model (with the loops) for the system PB-U13 S6

Appendix A S7

Equation A1

Table A1: Correction factor a_{Tg}

Appendix B S7

Equation B1 – B4

Additional information and Characterization

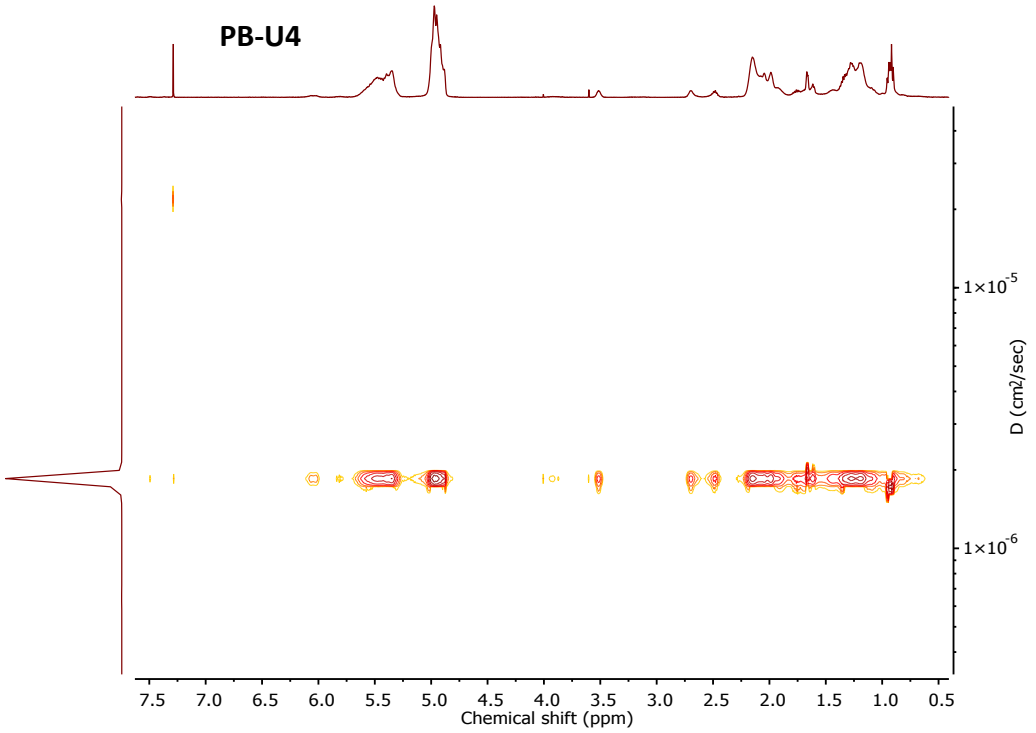

Figure S1. DOSY NMR spectrum of PB-U4.

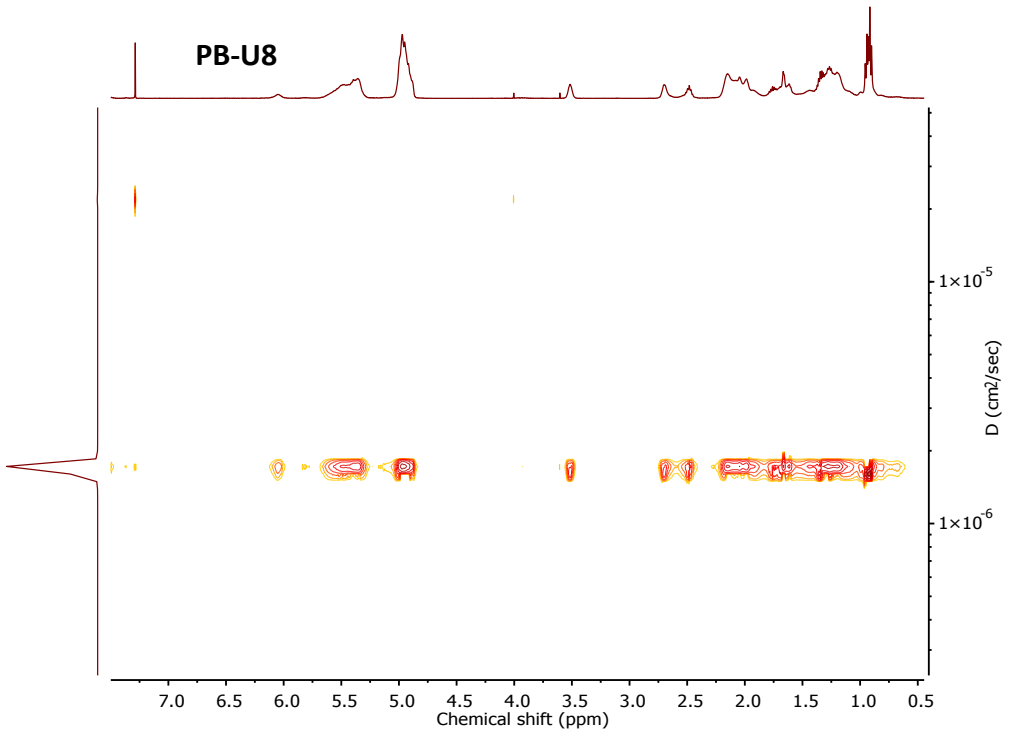

Figure S2. DOSY NMR spectrum of PB-U8.

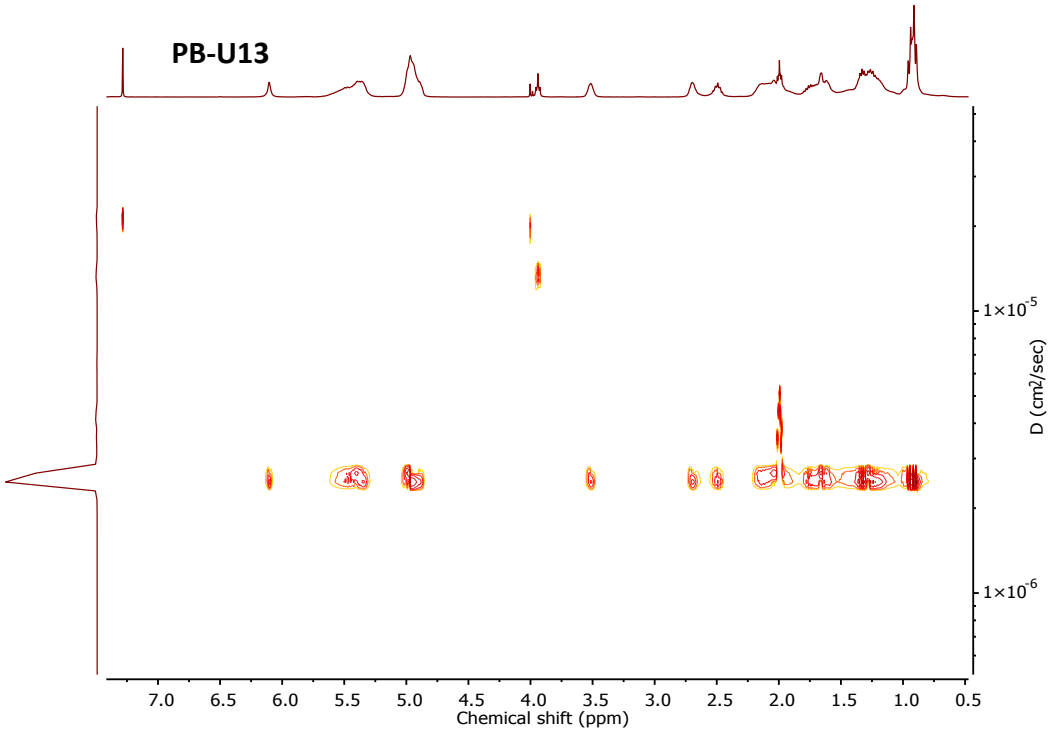

Figure S3. DOSY NMR spectrum of PB-U13.

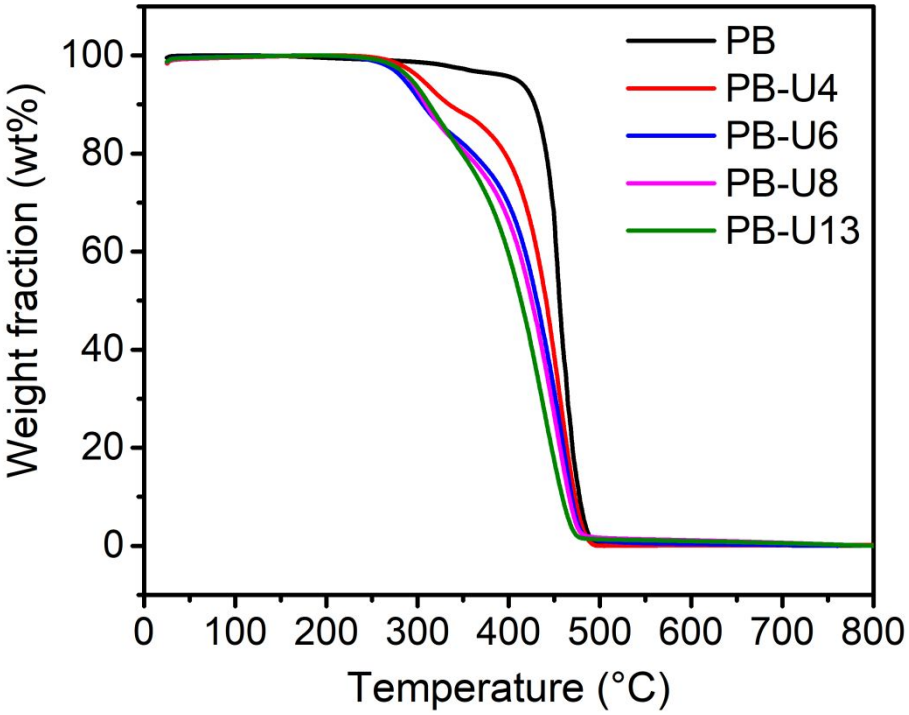

Figure S4. TGA curves of all PB-UPy polymers.

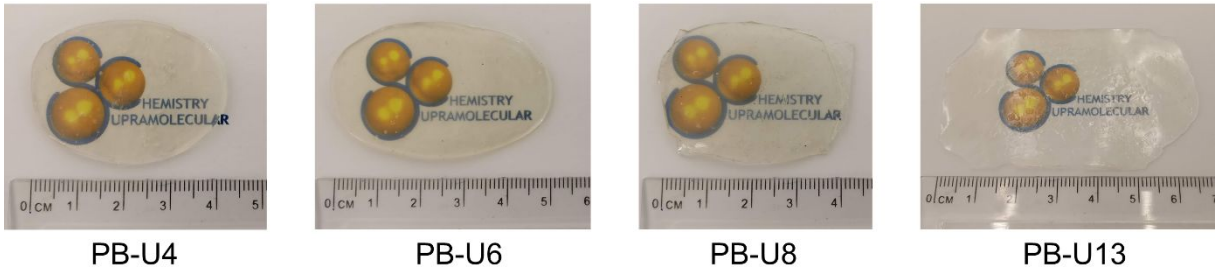

Figure S5. PB-UPy films obtained after compression molding.

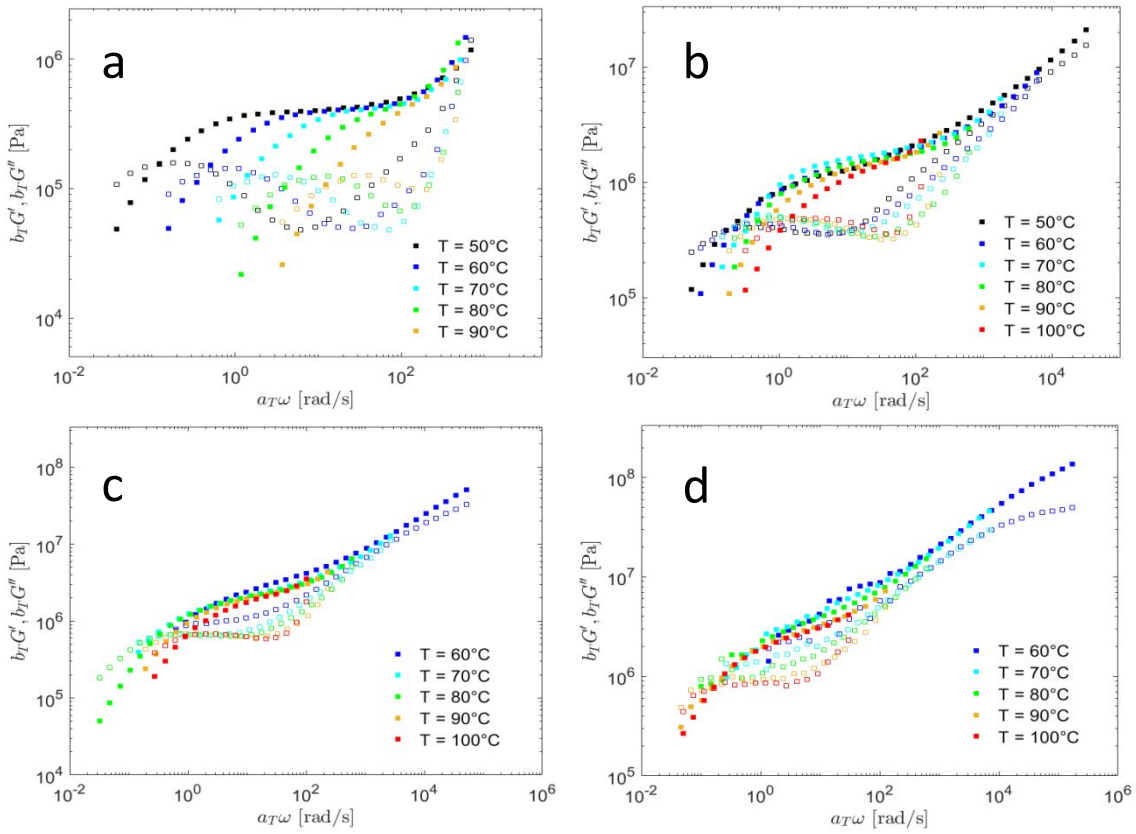

Figure S6. Test of time–temperature superposition of the storage and loss moduli, G' and G", of a) PB-U4 b) PB-U6 c) PB-U8 d) PB-U13 at $T_{ref} = 80°C$.

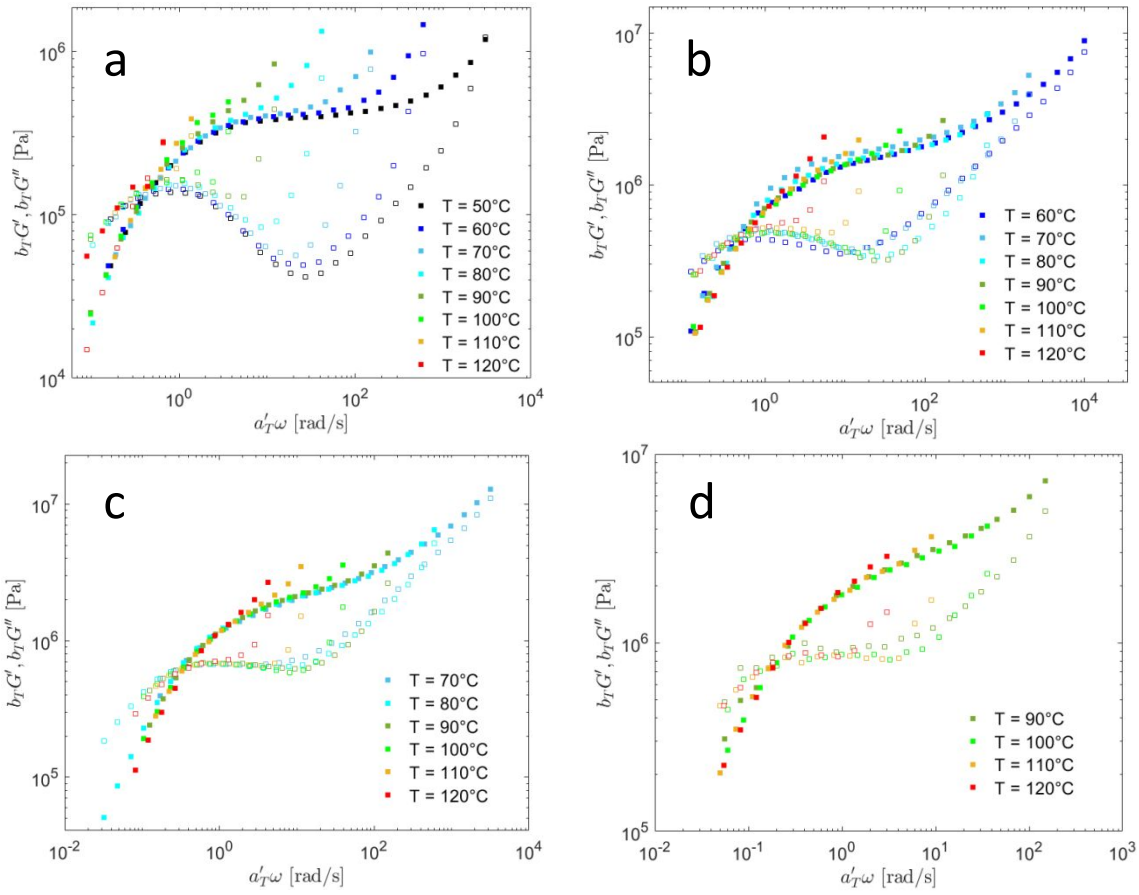

Figure S7. Test of time–temperature superposition of the storage and loss moduli, G' and G", of a) PB-U4 b) PB-U6 c) PB-U8 d) PB-U13 at $T_{ref} = 60°C$.

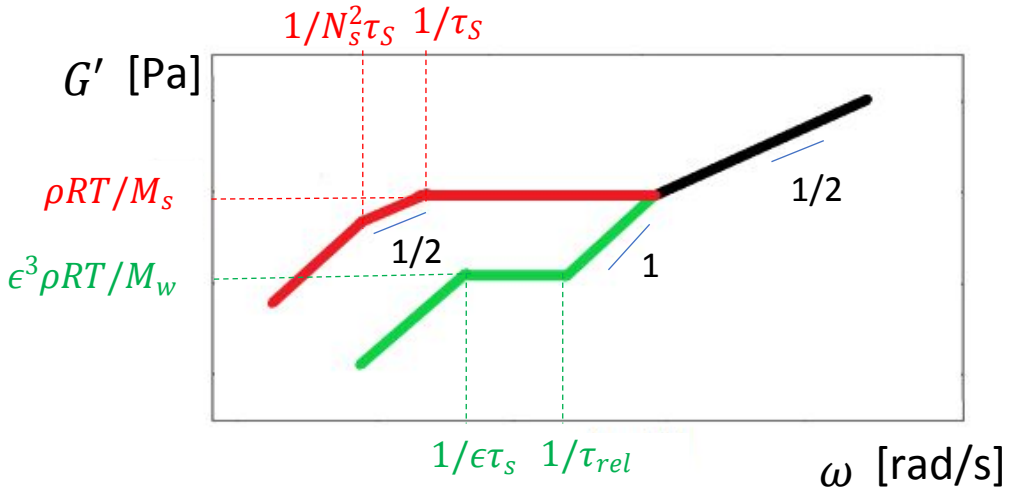

Figure S8. Scaling laws of the storage modulus for reversible network $(\epsilon > 1)$ and mixture of sol and gel $(0 < \epsilon < 1)$ (with mean-field percolation statistics).

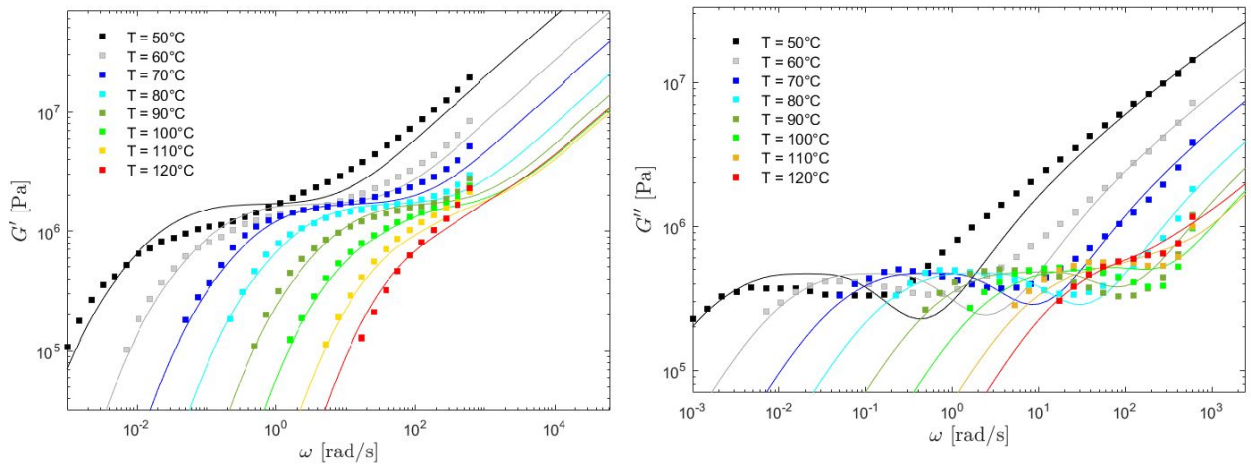

Figure S9. Predictions of the sticky Rouse model (with the loops) for the system PB-U6 at different temperatures. The relaxation has been computed based on the value in **Table 2**, and on equation 3) and 4). To account for temperature effect, the values of τ_0 and τ_s have been modified by the shift factors a_T and a_T' shown in **Figure 9.** The symbols are the experimental results and the solid lines are the predictions.

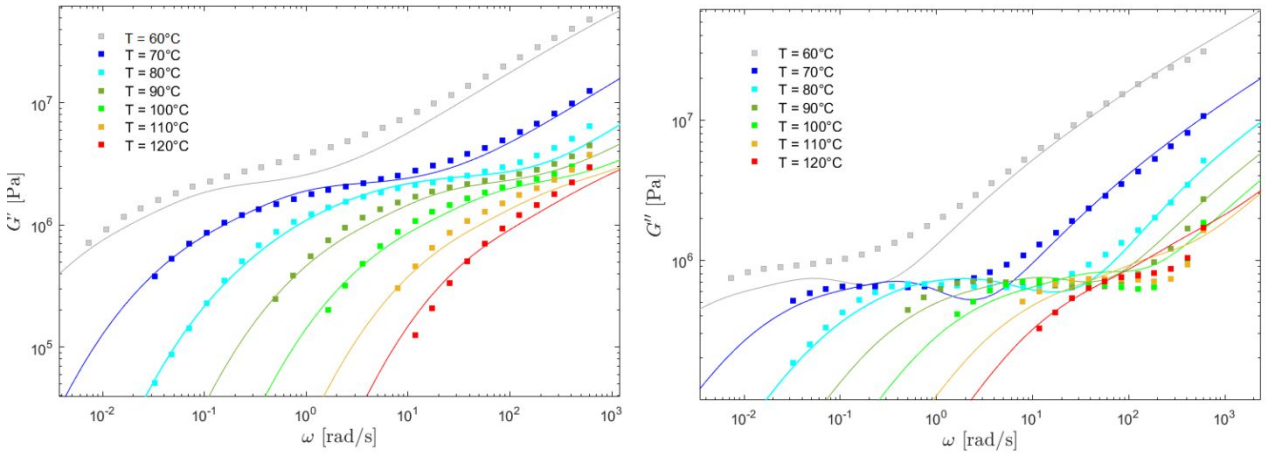

Figure S10. Predictions of the sticky Rouse model (with the loops) for the system PB-U8 at different temperatures. The relaxation has been computed based on the value in **Table 2**, and on equation 3) and 4). To account for temperature effect, the values of τ_0 and τ_s have been modified by the shift factors a_T and a_T' shown in **Figure 9.** The symbols are the experimental results and the solid lines are the predictions.

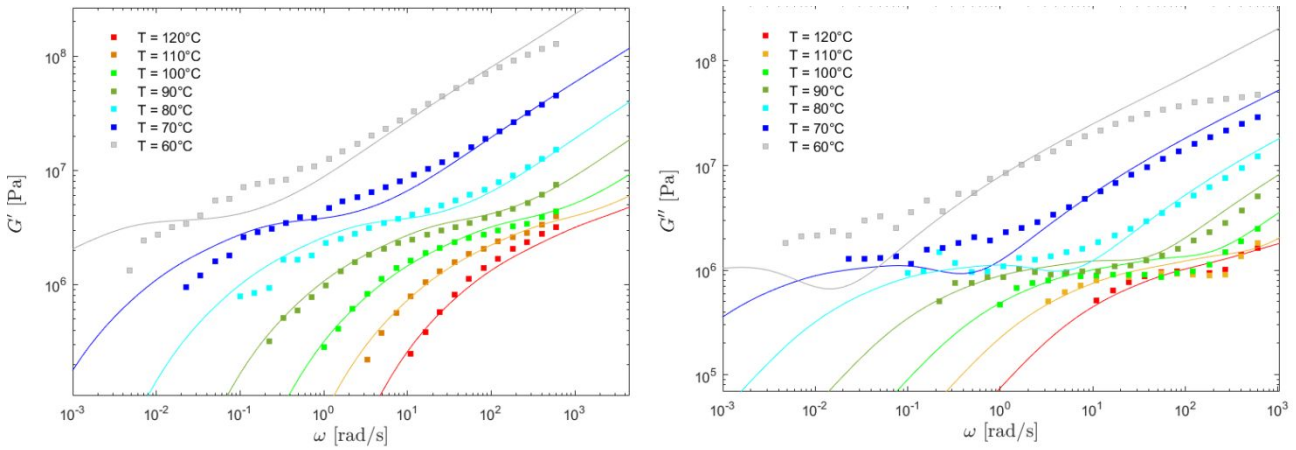

Figure S11. Predictions of the sticky Rouse model (with the loops) for the system PB-U13 at different temperatures. The relaxation has been computed based on the value in **Table 2**, and on equation 3) and 4). To account for temperature effect, the values of τ_0 and τ_s have been modified by the shift factors a_T and a_T' shown in **Figure 9.** The symbols are the experimental results and the solid lines are the predictions.

Appendix A

Due to the different glass transition temperatures of the systems, the horizontal shift factors of the PB – Upy systems are different and have a smaller temperature dependence with decreasing the UPy concentration. Indeed, as $T_{ref} - T_g$ increases, the activation energy decreases and so does the dependence of the relaxation times with the temperature. Despite this, as demonstrated by Wagner[1] and Liu *at al.*,[2] it is still possible to draw a mastercurve for the shift factors of all the systems. This can be done by multiplying the shift factors of the systems by a correction factor a_{T_g} which takes into account the effect of the different T_g. This shift a_{T_g} can be computed by a WLF-like equation:

$$log_{10}\, a_{T_g} = \frac{-c_1^0\,(T_{g,ref} - T_g)}{c_2^0 + (T_{g,ref} - T_g)}, \#(A1)$$

with the glass transition temperature T_g of the solutions and a reference glass transition temperature $T_{g,ref}$. The computed shift a_{T_g} are shown in Table 6. Here, PB – U13 is considered as the reference material.

Table A1. Correction factor a_{T_g}

	PB – U13	PB – U8	PB – U6
a_{T_g}	1	0.0791	0.0126

Appendix B

If a variable M is log-normally distributed, then its probability density function is given by

$$p(M = m) = \begin{cases} \frac{1}{m\sigma\sqrt{2\pi}} \exp\left(-\frac{(\ln m - \mu)^2}{2\sigma^2}\right), & m > 0 \\ 0, & \text{elsewhere} \end{cases} \#(B1)$$

The parameters μ and σ^2 can be expressed as a function of the mean $E[X]$ and the variance $Var[X]$ of the distribution in the following way.

$$\mu = \ln\left(\frac{E[X]^2}{\sqrt{E[X]^2 + Var[X]^2}}\right) \#(B2)$$

$$\sigma^2 = \ln\left(1 + \frac{Var[X]}{E[X]^2}\right) \#(B3)$$

The mean $E[X]$ is by definition equal to M_n and the variance $Var[X]$ can de deduced from

$$Var[X] = E[X^2] - E[X]^2 = M_w M_n - M_n^2 = M_n^2(\text{PDI} - 1) \#(B4)$$

As a consequence, one can model the molecular weight distribution from the values of the PDI and M_w.

References

(1) Wagner, M. H. Scaling relations for elongational flow of polystyrene melts and concentrated solutions of polystyrene in oligomeric styrene. *Rheol. Acta* , **2014**, *53,* 765–777

(2) Liu, C.-Y., He, J., Keunings, R. & Bailly, C. New Linearized Relation for the Universal Viscosity−Temperature Behavior of Polymer Melts. *Macromolecules* , **2006**, *39,* 8867–8869